Electronic Supplementary Material (ESI) for Physical Chemistry Chemical Physics.

Supplementary Information

Are hot charge transfer states the primary cause of efficient charge generation in polymer-fullerene organic photovoltaic devices? A Kinetic Monte Carlo study

Matthew L. Jones[1], Nigel Clarke[2], Reesha Dyer[1] and Chris Groves*[1]

[1]School of Engineering and Computing Sciences, Durham University, South Road, Durham, DH1 3LE, UK
[2]Department of Physics and Astronomy, Sheffield University, Hounsfield Road, S3 7RH, UK

Contents

*chris.groves@durham.ac.uk

S1 Cahn-Hilliard Morphology Generation

We use the Cahn-Hilliard theory, modified to account for surface interactions at the upper electrode, to model the spatio-temporal evolution of the blend composition. The equation of motion for the local volume fraction of donor, ϕ, can be written in the dimensionless form as:

$$\frac{\partial\phi(\vec{x},\tau)}{\partial\tau} = \nabla_x^2\left[\frac{1}{N_D(\chi-\chi_s)}\ln\phi - \frac{1}{N_A(\chi-\chi_s)}\ln(1-\phi) - \frac{2\chi\phi}{(\chi-\chi_s)} + \frac{2\phi-1}{36\phi^2(1-\phi)^2}(\nabla\phi)^2 - \frac{1}{18\phi(1-\phi)}\nabla^2\phi\right] \tag{1}$$

where N_A and N_D are the degrees of polymerisation of the acceptor and donor phases, χ is the Flory-Huggins interaction parameter, with χ_s its value on the spinodal curve. When $\chi > \chi_s$, the blend will undergo phase separation with diffusive dynamics described by the above equation. The first 3 terms arise from assuming that the free energy of the blend is described by the Flory-Huggins theory. The 4th and 5th terms on the right hand side arise from the energetic cost of gradients in composition. The dimensionless time and the space variables, τ and $\vec{x}$ are related to the real time, t and space, $\vec{r}$, through $\vec{x} = (|\chi-\chi_s|)^{\frac{1}{2}}\,\vec{r}/l$ and $\tau = N_A D\,(\chi-\chi_s)^2\,t/l^2$ so that to relate theory and experimental length and timescale, the blend must be characterised by the additional parameters, D, the mutual diffusion coefficient and l, the length of a statistical segment.

We solve the Cahn-Hilliard equation with periodic boundary conditions on a $128\times128\times127$ cubic lattice using a finite difference scheme. Initially the composition of the blend is uniform throughout the lattice, such that at $\tau = 0, \phi(\vec{x},0) = \phi_0 + \delta$, where δ is a uniformly distributed random variable in the range $-0.01 < \delta < 0.01$. For the D:A morphology, we use $\phi_0 = 0.5$, $\chi = 0.0654$ and $N_A = N_D = 50$, such that $\chi_s = 0.04$, with reduced time and space steps of $\Delta\tau = 1.25\times10^{-4}$ and $\Delta x = 0.5$. For the Mx:Ag morphology, we use $\phi_0 = 0.4$, $\chi = 0.9$, $N_A = 30$ and $N_D = 1$, such that $\chi_s = 0.875$, with reduced time and space steps of $\Delta\tau = 1.0\times10^{-5}$ and $\Delta x = 0.5$. These parameters are chosen to ensure we mimic a deep quench into the two-phase region, which is expected to give rise to nanoscale morphologies typically observed in photovoltaic polymer blends.

S2 Morphology Characterisation

Fig. 1	Blend	Ratio	d	Proportions		FF at	PCE
				D/Mx	A/Ag	r = 4 nm	%
a)	D:A	1:1	6.63 nm	0.50066	0.49934	0.25140	0.22870
b)	Mx:Ag	2:3	4.72 nm	0.96134	0.03866	0.29239	0.01360
c)	Mx:Ag	2:3	4.23 nm	0.73501	0.26499	0.26923	0.07880
d)	Mx:Ag	2:3	6.79 nm	0.60402	0.39598	0.27374	0.12740
e)	Mx:Ag	2:3	10.28 nm	0.58899	0.41101	0.27878	0.13540

Table 1: A table of the key features and performance of the morphologies used in this investigation.

Table 1 shows the key features of the morphologies used in this investigation, such as blend ratio and the average domain size (d). Note that D:A represents a donor:acceptor blend with regions of pure donor (D) and pure acceptor (A). Mx:Ag describes a mixed:acceptor blend containing domains of aggregated fullerene (Ag) surrounded by a large mixed phase where both polymers and fullerenes are present (Mx). The fill factors and power conversion efficiencies (PCE) are shown for comparison.

S3 Simulation Parameters

Simulation Parameter	Value
Material Parameters	
Acceptor LUMO	$-3.9\,\mathrm{eV}$
Donor HOMO	$-5.3\,\mathrm{eV}$
Cathode Workfunction	$-4.2\,\mathrm{eV}$
Anode Workfunction	$-5.0\,\mathrm{eV}$
Photoabsorption Coefficient	$1.3 \times 10^6\,\mathrm{m}^{-1}$
Photoinjection rate	$6.27 \times 10^6\,\mathrm{s}^{-1}$
Dielectric Constant, ϵ	3
Charge Parameters	
Applied Electric Field (GPS simulations), F	$5 \times 10^6\,\mathrm{V\,m}^{-1}$
Recombination Rate, k_r	$1 \times 10^9\,\mathrm{s}^{-1}$
Exciton Lifetime, τ_{PL}	500 ps
Forster Radius, R_{F}	4.3 nm
Hopping Parameters	
Marcus Hopping Prefactor (hole), $v_{0,h}$	$1 \times 10^{11}\,\mathrm{s}^{-1}$
Marcus Hopping Prefactor (electron), $v_{0,e}$	$1 \times 10^{11}\,\mathrm{s}^{-1}$
Reorganization Energy, E_r	0.25 eV
Gaussian DoS width, σ	50 meV
Photoinjection Parameters	
Incident Flux	$100\,\mathrm{mW\,cm}^{-2}$
Incident Wavelength	500 nm
Temperature	298 K

Table 2: Parameters used in the Monte Carlo Simulations.

Table 2 describes the fiducial simulation parameters used in this investigation. All simulations used this parameter set unless otherwise specified. These values were chosen to approximate the simulations to a polymer:fullerene blend device such as P3HT:PC_{61}BM. The photoinjection parameters approximate to an air mass index of AM1.5.

S4 Additional Simulation Characteristics

System Name	Exciton Dissociation Efficiency	Charge Collection Efficiency
D:A, $r = 1$, Fig 1a)	0.99566	0.03273
D:A, $r = 2$, Fig 1a)	0.99564	0.04827
D:A, $r = 4$, Fig 1a)	0.99578	0.16120
D:A, $r = 6$, Fig 1a)	0.99614	0.30310
D:A, $r = 8$, Fig 1a)	0.99576	0.41491
D:A, $r = 10$, Fig 1a)	0.99601	0.50521
Mx:Ag, $\beta = 0.039$, Fig 1b)	1.00000	0.03445
Mx:Ag, $\beta = 0.266$, Fig 1c)	0.99994	0.06927
Mx:Ag, $\beta = 0.396$, Fig 1d)	0.99883	0.08258
Mx:Ag, $\beta = 0.411$, Fig 1e)	0.99651	0.09402

Table 3: Some additional calculated efficiencies from various input simulations described in the main text.

Table 3 shows that the exciton dissociation efficiency is $> 99\%$ for all simulations, indicating that very few photoinjected excitons decayed before reaching a heterojunction in the $d = 7\,\text{nm}$ optimised morphologies. The remaining charge carrier losses are due to geminate and non-geminate recombination.

S5 Alternative HCT state methodology

Here, we describe an alternative HCT state methodology within the device. In the main text for Mx:Ag morphologies, HCT states are only formed at the Mx:Ag interface and not throughout the mixed phase. We call this 'aggregate' separation. Here, we demonstrate the effect of 'general' separation, where HCTs are produced at *every* exciton dissociation, even in the Mixed Phase.

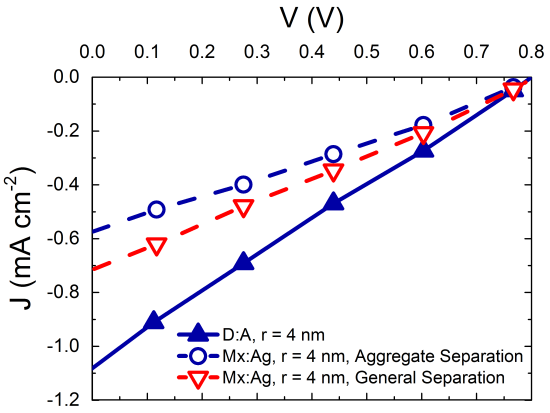

Figure S1: A comparison between the different HCT state methodologies

Figure S1 shows the J-V curves from figure 4 in the main text (blue), for $d = 7\,\text{nm}$ D:A (solid lines and symbols) and Mx:Ag (dashed lines and open symbols) morphologies for $k_r = 1 \times 10^9\,\text{s}^{-1}$ and $r = 4\,\text{nm}$. Also included is the J-V data for the same morphology with 'general' separation activated (red).

The performance increase awarded by permitting HCTs ubiquitously is insufficient to compete with the corresponding donor-acceptor morphology. This suggests that the presence of the mixed phase limits the efficacy of HCTs too severely for them to be a unique precursor to high IQEs in polymer:fullerene devices.